

Toward Architecture-Agnostic Local Control of Posterior Collapse in VAEs

Hyunsoo Song¹ Seungwhan Kim² Seungkyu Lee³

Abstract

Variational autoencoders (VAEs), one of the most widely used generative models, are known to suffer from posterior collapse, a phenomenon that reduces the diversity of generated samples. To avoid posterior collapse, many prior works have tried to control the influence of regularization loss. However, the trade-off between reconstruction and regularization is not satisfactory. For this reason, several methods have been proposed to guarantee latent identifiability, which is the key to avoiding posterior collapse. However, they require structural constraints on the network architecture. For further clarification, we define local posterior collapse to reflect the importance of individual sample points in the data space and to relax the network constraint. Then, we propose *Latent Reconstruction* (LR) loss, which is inspired by mathematical properties of injective and composite functions, to control posterior collapse without restriction to a specific architecture. We experimentally evaluate our approach, which controls posterior collapse on varied datasets such as MNIST, fashionMNIST, Omniglot, CelebA, and FFHQ.

1. Introduction

VAEs (Variational auto-encoders) are popular generative latent models, which have been used in various applications such as representation learning, manifold learning, and dimension reduction. However, they have suffered from a chronic posterior collapse problem, which reduces the diversity of outputs. Although many studies (Lucas et al., 2019a) (Lucas et al., 2019b) (Dai et al., 2020) (Razavi et al., 2019) (Clapham & Grzes, 2023) (Rueck-

ert et al., 2023) (Wang et al., 2021) (Kinoshita et al., 2023) have tried to analyze and address it, some ambiguity and limitations remain. Regularization loss is highly related to the posterior collapse phenomenon. Thus, tuning the importance (β) (Higgins et al., 2017) of regularization loss has been widely used. From a theoretical perspective, many works, such as (Ichikawa & Hukushima, 2024) report that posterior collapse is unavoidable once β exceeds a specific value. However, the optimal point on the trade-off curve provided by these methods has been regarded as unsatisfactory. Minimizing the ELBO objective in VAEs does not necessarily ensure both accurate latent inference and faithful data reconstruction (Zhao et al., 2019) (Dai et al., 2021). A recent study (Song et al., 2024) similarly argues that posterior collapse arises from optimization dynamics rather than solely from KL imbalance. A study (Wang et al., 2021) has shown that preserving the identifiability of the latent variable, which is key to avoiding posterior collapse, can be achieved by implementing an injective decoder based on a *Brenier map*. Ensuring latent variable identifiability makes the ELBO optimum more reliable. However, they only avoid the extreme case of posterior collapse, and the decoder architecture is restricted to ICNN (Amos et al., 2017). Therefore, later work (Kinoshita et al., 2023) (Kinoshita & Toyoizumi, 2024) explores the control of posterior collapse under more general conditions. However, the global Lipschitz condition may be strong for ideal latent models. In addition, the choice of architecture is still restricted to be a *Brenier map*.

In this work, we define posterior collapse in more general and relaxed manner. In addition, we show that ensuring *locally $L(z)$ -bi-Lipschitz continuity* of the encoder or decoder helps to avoid posterior collapse. To realize this condition in an architecture-agnostic manner, we propose LRVAE (Latent Reconstruction VAE), which is a loss-based approach that implicitly encourages latent identifiability through a *symmetric reconstruction loss* composed of data reconstruction and latent reconstruction terms. Our method remains broadly applicable, offering high practical utility. We also evaluate our models, which are implemented based on both shallow and deep (Child, 2020) VAE architectures as the backbone, with measuring metrics related to posterior collapse and showing responses w.r.t. tiny latent vector differences. In our experiments, MNIST (Deng, 2012), fashion-

¹Innovation Center for Industrial Mathematics, National Institute for Mathematical Sciences, Seongnam-si, Republic of Korea ²Interdisciplinary Program in Artificial Intelligence, Seoul National University, Seoul-si, Republic of Korea ³Department of Computer Science and Engineering, KyungHee University, Yongin-si, Republic of Korea. Correspondence to: Hyunsoo Song <song@nims.re.kr>, Seungkyu Lee <seungkyu@khu.ac.kr>.

MNIST (Xiao et al., 2017), Omniglot (Lake et al., 2015), CelebA (Liu et al., 2015), and FFHQ-256 (Karras et al., 2019) datasets are used. Experimental results show that VAEs effectively avoid posterior collapse, securing generation output diversity even at around tiny latent differences.

2. Local Posterior Collapse and Local bi-Lipschitz Continuity

A pioneer work (Wang et al., 2021) defines posterior collapse as the phenomenon in which the learned posterior becomes non-informative or input-independent, leading to a loss of latent identifiability. They define posterior collapse more strictly as the equality $p_{\hat{\theta}}(z|x) = p(z)$, where $p_{\hat{\theta}}(z|x)$ is the true posterior under the optimized parameter $\hat{\theta}$. However, this definition may be overly strict as they do not tolerate even small input-dependent variations in the posterior distribution. For this reason, a later work (Kinoshita et al., 2023) uses the ϵ -posterior collapse as $d(q_{\hat{\varphi}}(z|x), p(z)) \leq \epsilon$ to relax the condition. However, a globally applied constant threshold ϵ might still impose an overly restrictive condition. Therefore, relaxation would be required. For example, a previous work (Lucas et al., 2019b) defines (ϵ, Δ) -posterior collapse as a probabilistic representation $\mathbb{P}_{x \sim P_X(x)}[D_{KL}(q_{\hat{\varphi}}(z|x), p(z)) < \epsilon] \geq 1 - \Delta$. Another work (Razavi et al., 2019) loosely defines posterior collapse as the KL divergence $D_{KL}(q(z|x) || p(z))$ approaches zero, where $q(z|x)$ is the approximate posterior and $p(z)$ is the prior. We summarize the posterior collapse definitions in Appendix B.

Despite many definitions having been proposed, some ambiguities remain. Empirical datasets rarely exhibit uniform conditional complexity: some inputs x can be reconstructed with negligible latent information, whereas others require a substantial mutual-information budget. A single global tolerance ϵ for detecting posterior collapse $\text{KL}[q_{\varphi}(z | x) || p(z)] \leq \epsilon$ is therefore ill-suited: it *under-detects* collapse in high-entropy regions and *over-penalises* low-entropy ones. To align the collapse test with this heterogeneous geometry, we introduce an input-dependent threshold $\epsilon : x \rightarrow [0, \infty)$. The resulting $\epsilon(x)$ -posterior-collapse criterion (i) preserves information where the decoder is sensitive, (ii) allows stronger compression where it is benign, and (iii) integrates naturally with the local bi-Lipschitz analysis developed in the sequel.

Definition 2.1 ($\epsilon(x)$ -Posterior Collapse). Let $X = \{x_1, \dots, x_n\} \subset \mathbb{R}^D$ denote a finite dataset, and let $\mathcal{X} \subset \mathbb{R}^D$ be a compact domain that includes the support of the empirical data distribution. We assume the data distribution p_X as the uniform mixture of Dirac delta measures centered at the data points, i.e., $p_X(x) := \frac{1}{n} \sum_{i=1}^n \delta_{x_i}(x)$.

We say that a model exhibits $\epsilon(x)$ -posterior collapse if,

for both true posterior $p_{\hat{\theta}}(z|x)$ and approximate posterior $q_{\hat{\varphi}}(z|x)$, the following holds:

$$\sup_{\rho \in \{p_{\hat{\theta}}, q_{\hat{\varphi}}\}} d(\rho(z|x), p(z)) \leq \epsilon(x), \quad \forall x \in \mathcal{X}. \quad (1)$$

where $d(\cdot, \cdot)$ is a divergence (e.g., KL divergence or Wasserstein distance), $\hat{\theta}$ and $\hat{\varphi}$ denote optimized parameters of decoder and encoder, and $\epsilon : \mathcal{X} \rightarrow [0, \infty)$ is a threshold function satisfying:

1. **(Maximum on data)** There exists a constant $\epsilon_{\max} > 0$ such that

$$\epsilon(x) = \epsilon_{\max} \quad \text{for all } x \in X.$$

2. **(Monotonic decay)** For all $x, x' \in \mathcal{X}$,

$$\text{dist}(x, X) < \text{dist}(x', X) \Rightarrow \epsilon(x) \geq \epsilon(x').$$

3. **(Asymptotic decay)** As x moves away from the dataset,

$$\lim_{\text{dist}(x, X) \rightarrow \infty} \epsilon(x) = 0.$$

Here, $\text{dist}(x, X) := \min_{1 \leq i \leq n} \|x - x_i\|$ denotes the Euclidean distance to the dataset. This definition (2.1) generalizes the notion of ϵ -posterior collapse (Kinoshita et al., 2023) by introducing a pointwise threshold function $\epsilon(x)$ instead of a constant. This functional form allows greater flexibility by tolerating small deviations from the prior in less informative regions of the input space (e.g., noisy or unstructured images), thereby avoiding overly restrictive constraints on the model behavior. In contrast, previous works adopted a constant ϵ determined via heuristic tuning. However, such global constants are inherently ambiguous, as the optimal threshold depends on the model capacity, data distribution, and the specific notion of collapse used. Therefore, in this work, we do not assume any explicit or fixed form for $\epsilon(x)$, allowing it to reflect the local informativeness of each input. The approximate posterior collapse can also be defined in the same manner (see Appendix B). In our work, the true posterior and the approximate posterior converge to the same distribution by using symmetric reconstruction loss, as shown in D.1. In addition, we define the posterior collapse for both approximate posterior and true posterior. Because the convergence of the encoder and decoder is interdependent; if either collapses, they cannot be trained correctly. The inference gap, which is the difference between these two posteriors, is intractable but must be minimized to justify the existence of the encoder. This implies that both types of posterior collapse must be avoided.

Definition 2.2 ($L(z)$ -bi-Lipschitz continuity of decoder with probability $1 - \zeta$). Let $D_{\theta} : \mathcal{Z} \rightarrow \mathcal{X}$ be the decoder and

let $p(z)$ be a prior on \mathcal{Z} . For any confidence level (a scalar) $\zeta \in (0, 1)$ define the radius R as:

$$R_\zeta := \inf\{R > 0 \mid \Pr_{Z \sim p}(\|Z\| \leq R) \geq 1 - \zeta\}.$$

We say that D_θ is $L(z)$ -bi-Lipschitz with probability $1 - \zeta$ if there exist measurable functions

$$r : \mathcal{Z} \rightarrow (0, \infty), \quad L : \mathcal{Z} \rightarrow [1, \infty)$$

such that for every $z \in \mathcal{Z}$ with $\|z\| \leq R_\zeta$ and for all $z_1, z_2 \in B(z, r(z))$,

$$\frac{1}{L(z)} \|z_1 - z_2\| \leq \|D_\theta(z_1) - D_\theta(z_2)\| \leq L(z) \|z_1 - z_2\|. \quad (2)$$

Moreover, the following global bounds (within the effective support) are finite and strictly positive:

$$r_{\min}^{(\zeta)} := \inf_{\|z\| \leq R_\zeta} r(z) > 0, \\ L_{\max}^{(\zeta)} := \sup_{\|z\| \leq R_\zeta} L(z) < \infty.$$

By this definition, we represent the bi-Lipschitz continuity locally.

Theorem 2.3 (Gaussian VAE: $L(z)$ -bi-Lipschitz avoids $\epsilon(x)$ -posterior collapse with probability $1 - \zeta$). *Fix a confidence level $\zeta \in (0, 1)$ and let radius R_ζ be defined as in Definition 2.2. Let the prior be $p(z) = \mathcal{N}(0, I)$ and the likelihood*

$$p(x | z) = \mathcal{N}(D_\theta(z), \sigma^2 I).$$

Assume the decoder D_θ is \mathcal{C}^2 and $L(z)$ -bi-Lipschitz with probability $1 - \zeta$. Consider any $x \in \mathcal{X}$ for which there exists z_0 satisfying

$$\|z_0\| \leq R_\zeta, \quad D_\theta(z_0) = x.$$

Define

$$\Sigma = \left(I + \frac{1}{\sigma^2} J_D(z_0)^\top J_D(z_0) \right)^{-1}, \\ \kappa_{\min} = \sigma_{\min}(J_D(z_0)) \geq \frac{1}{L(z_0)} > 0.$$

Then, under the Laplace approximation,

$$p(z | x) \approx \mathcal{N}(z_0, \Sigma) \\ \Rightarrow D_{\text{KL}}(p(z | x) \| p(z)) \geq \frac{C}{2} \log\left(1 + \frac{\kappa_{\min}^2}{\sigma^2}\right) > 0.$$

Consequently, with probability at least $1 - \zeta$ over $x \sim p_{\text{data}}$, no $\epsilon(x) < \frac{C}{2} \log(1 + \kappa_{\min}^2/\sigma^2)$ can satisfy Definition 2.1. The proof of this Theorem is provided in Appendix A.1.

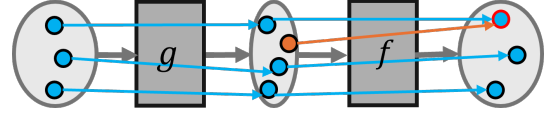


Figure 1: A sample injective/composite function where g is injective but f is not when $f \cdot g$ is injective: The orange dot on latent space has same output with other latent vector.

3. Method: Latent Reconstruction

We propose the Latent Reconstruction (LR) loss (\mathcal{L}_{LR}) as an additional loss term for ELBO objectives as follows:

$$\mathcal{L}_{LR} = \mathbb{E}_{p_\theta(x|z)}[-\log q_\varphi(z|x)] = \|E_{\varphi, \mu}(D_\theta(z)) - z\|^2,$$

where $q_\varphi(z|x)$ is assumed to be a normal distribution, and $E_{\varphi, \mu}$ denotes the encoder function that has an output μ (mean of z) before latent random reparameterization.

If a composite function $f \cdot g$ is injective, then g must be injective, but f is not necessarily so. Figure 1 represents an example where g is an injective but f is not, even though $f \cdot g$ is injective. We apply this mathematical property to the VAE architecture.

Our key idea is to *stochastically* enforce that the composite map $E_{\varphi, \mu} \circ D_\theta$ approximates the identity on latent draws, i.e.,

$$E_{\varphi, \mu}(D_\theta(z)) \approx z.$$

Driving down the latent reconstruction (LR) loss tightens this identity approximation, pressuring D_θ to admit a data-driven inverse realized by $E_{\varphi, \mu}$.

In particular, DR and LR loss minimization promotes **relaxed latent identifiability that goes beyond mere injectivity**. While precisely defining this resulting state is challenging, we interpret it as locally ($L(z)$) bi-Lipschitz behavior. This is visualized in Figure 2.

Theorem 3.1 (High-Probability Locally Bi-Lipschitz under Piecewise-Linear Networks). *Fix confidence levels $\zeta, \rho \in (0, 1)$ and let radius R_ζ be defined as in Definition 2.2. Let $D_\theta : \mathbb{R}^C \rightarrow \mathbb{R}^D$ and $E_\varphi : \mathbb{R}^D \rightarrow \mathbb{R}^C$ be feed-forward networks built from affine layers and piecewise-linear activations (e.g. ReLU, LeakyReLU).*

Draw $Z \sim p(z)$ and denote the effective-support event $\mathcal{E}_\zeta := \{\|Z\| \leq R_\zeta\}$, which satisfies $\Pr(\mathcal{E}_\zeta) \geq 1 - \zeta$. On \mathcal{E}_ζ there exists a radius $r > 0$ such that the activation pattern of every piecewise-linear unit is fixed on $B(Z, r)$. Hence D_θ and $E_\varphi \circ D_\theta$ restrict to affine maps on $B(Z, r)$ and are therefore \mathcal{C}^1 there.

Define the random variables

$$A := \|J_D(Z)\|_\sigma, \quad B := \|J_{E \circ D}(Z) - I\|_\sigma,$$

and assume $\mathbb{E}[A^2] < \infty$ and $\mathbb{E}[B^2] < \infty$.

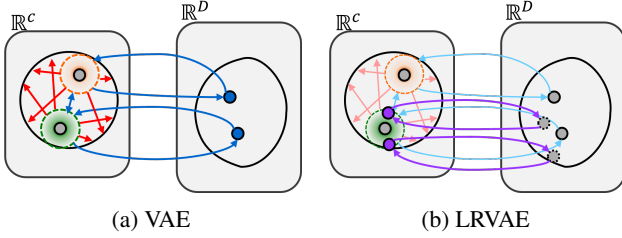


Figure 2: Influence of ELBO objectives of VAE and our LRVAE in latent space(\mathbb{R}^C) and data space(\mathbb{R}^D): Regularization loss(Red arrows) leads latent variables to be close to prior. Reconstruction loss(Blue Arrows) leads latent variables identifiable from each other against regularization loss. However, reconstruction loss does not lead latent point to be identifiable from its distribution. The reconstruction loss secure latent identifiability only to distinguish data point. Whereas, Our latent reconstruction loss(Violet arrows), which is an additional term, directly secures identifiability of whole latent variable.

Then for any $\varepsilon \in (0, 1)$ there exist thresholds $\tau_r, \tau_l > 0$ (depending on ε, ϱ) such that, if

$$\mathcal{L}_{\text{DR}}(\theta, \varphi) \leq \tau_r, \quad \mathcal{L}_{\text{LR}}(\theta, \varphi) \leq \tau_l,$$

the following holds with probability at least $1 - \zeta - \varrho$ over $Z \sim p$:

There exist constants $L_f < \infty$ and $\eta < 1$ such that

$$A \leq L_f, \quad B \leq \eta,$$

and consequently D_θ is bi-Lipschitz on the ball $B(Z, r)$ with constant

$$L = \max\left(L_f, \frac{1}{1-\eta}\right),$$

i.e. for all $z_1, z_2 \in B(Z, r)$,

$$(1-\varepsilon) \|z_1 - z_2\| \leq \|D_\theta(z_1) - D_\theta(z_2)\| \leq (1+\varepsilon) \|z_1 - z_2\|.$$

For the proof of this Theorem, see Appendix A.2. As a result, minimizing the proposed LR loss with the conventional DR loss can help avoid posterior collapse according to our definition.

Applicability to Both Piecewise-Linear and Smooth Activations. Theorem 3.1 holds for networks built with piecewise-linear activations (e.g. ReLU or LeakyReLU), where each activation region is exactly affine and thus \mathcal{C}^1 locally, and for networks using globally smooth \mathcal{C}^1 activations (e.g. SiLU, GELU, or Tanh), where the Jacobians J_D and $J_{E \circ D}$ are continuous on all of \mathbb{R}^C . In both cases, for any $\varrho, \varepsilon \in (0, 1)$ and sufficiently small DR and LR losses, there exist constants $L_f < \infty$, $\eta < 1$ and a radius $r > 0$ such that

with probability at least $1 - \varrho$, D_θ is locally bi-Lipschitz on $B(Z, r)$ with bi-Lipschitz constant

$$L = \max\left(L_f, \frac{1}{1-\eta}\right).$$

as in Theorem 3.1.

3.1. Implementation Details

Additionally, we adopt objectives with a weight α on our proposed term(LR) to optimize the model. The total objectives are represented as:

$$\mathcal{L}_{\text{total}}(x) = \beta D_{\text{KL}}(q_\varphi(z|x_i) || p(z)) + \mathbb{E}_{q_\varphi(z|x_i)} [-\log p_\theta(x_i|z)] + \alpha \mathbb{E}_{p_\theta(x|z_i)} [-\log q_\varphi(z_i|x)],$$

where β (Higgins et al., 2017) is the weight of the regularization loss. Because a latent variable usually has a simple distribution and a low dimension, latent reconstruction loss is easier to optimize than data reconstruction loss. The global optimum of latent reconstruction loss would exist in infinitely many areas. We suppose that most of them could be bad local minima of the total loss. Therefore, using an arbitrary weighting or naive training scheme can lead to local minima where only latent reconstruction is satisfied, especially in the early stages of training. To mitigate this risk, we use a warm-up strategy that gradually increasing α from 0 to a specific hyperparameter α_T , as described in each experiment. i.e., $\alpha := \alpha_t$ is used when the epoch index is $t \in \{0, \dots, T\}$.

4. Experiments

In our experiments, we focus on showing that posterior collapse can be controlled by proposed latent reconstruction loss.

Model	β	L	α_T	AU	KL	MI
VAE	1.0	-	-	0.13	7.10	3.84
SA-VAE	1.0	-	-	0.13	6.89	3.77
Lagging VAE	1.0	-	-	0.16	7.27	3.79
β -VAE	0.1	-	-	0.22	18.12	3.93
β -VAE	0.2	-	-	0.19	13.78	3.84
β -VAE	0.4	-	-	0.16	10.54	3.91
LIDVAE	1.0	0	-	0.42	25.15	3.88
IL-LIDVAE	1.0	0.1	-	0.80	49.54	3.92
IL-LIDVAE	1.0	0.2	-	0.72	54.68	3.93
IL-LIDVAE	1.0	0.4	-	0.72	67.35	3.92
LRVAE(ours)	0.1	-	1.0	0.95	45.23	3.86
LRVAE(ours)	0.2	-	1.0	0.93	33.36	3.99
LRVAE(ours)	1.0	-	1.0	0.41	12.41	3.77

Table 1: Quantitative evaluation on fashionmnist dataset

First, we evaluate and compare several models using quantitative metrics(AU, KL, MI) (Wang et al., 2021)(Kinoshita

Model	β	L	α_T	AU	KL	MI
VAE	1.0	-	-	0.16	8.69	3.96
SA-VAE	1.0	-	-	0.19	9.26	3.91
Lagging VAE	1.0	-	-	0.19	9.18	3.84
β -VAE	0.1	-	-	0.68	32.40	3.90
β -VAE	0.2	-	-	0.38	23.48	3.93
β -VAE	0.4	-	-	0.33	16.52	3.92
LIDVAE	1.0	0	-	0.94	50.70	3.90
IL-LIDVAE	1.0	0.1	-	0.96	70.19	3.85
IL-LIDVAE	1.0	0.2	-	0.88	69.59	3.90
IL-LIDVAE	1.0	0.4	-	0.94	89.83	3.89
LRVAE(ours)	0.1	-	0.4	1.00	45.20	3.84
LRVAE(ours)	0.2	-	0.4	0.99	32.80	3.90
LRVAE(ours)	1.0	-	0.4	0.22	11.92	3.91
LRVAE(ours)	1.0	-	1.0	0.66	14.85	3.90

Table 2: Quantitative evaluation on MNIST dataset

Model	β	L	α_T	AU	KL	MI
VAE	1.0	-	-	0.06	2.32	2.11
SA-VAE	1.0	-	-	0.09	2.80	2.45
Lagging VAE	1.0	-	-	0.06	2.23	2.03
β -VAE	0.1	-	-	0.85	30.05	3.93
β -VAE	0.2	-	-	0.52	18.24	3.86
β -VAE	0.4	-	-	0.22	11.33	3.91
LIDVAE	1.0	0	-	0.99	15.02	3.85
IL-LIDVAE	1.0	0.2	-	0.93	26.24	3.88
IL-LIDVAE	1.0	0.8	-	0.97	109.73	3.93
IL-LIDVAE	1.0	1.0	-	0.45	120.17	3.88
LRVAE(ours)	1.0	-	0.1	0.13	3.68	2.76
LRVAE(ours)	1.0	-	0.4	0.77	6.18	3.26
LRVAE(ours)	1.0	-	1.0	0.86	7.84	3.32

Table 3: Quantitative evaluation on Omniglot dataset

et al., 2023). Results are shown in Table 1, 2, 3, and 4. Models used in the comparison are VAE(Kingma & Welling, 2013), SA-VAE(Kim et al., 2018), Lagging VAE(He et al., 2019), β -VAE(Higgins et al., 2017), LIDVAE(Wang et al., 2021), and IL-LIDVAE(Kinoshita et al., 2023).

β denotes weight of regularization loss, while α_T denotes final weight of our proposed latent reconstruction loss which is warm-up from 0 to described value through linear increase from epoch 0 to end(100). L denotes inverse Lipschitz value of IL-LIDVAE. Activation Unit(AU) denotes ratio of activated latent channels which is calculated as $AU = \sum_c^C \mathbb{1}\{Cov_{p(x)}(\mathbb{E}_{q(z|x)}[z_{(c)}]) \geq \varepsilon\}$, where $z_{(c)} = \{z_{i,c}, \dots, z_{i,c}\}$ is the c -th dimension of the latent variable z for the N validation data points. $\mathbb{1}$ denotes an indicator function. Since deactivated channels are almost completely unidentifiable (related to ε), AU serves as a meaningful metric for estimating the upper bound of latent identifiability. Bigger AU is better. KL denotes sample-

Model	β	L	α_T	AU	KL	MI
VAE	1.0	-	-	0.47	40.87	3.85
SA-VAE	1.0	-	-	0.67	45.16	3.88
Lagging VAE	1.0	-	-	0.63	42.46	3.96
β -VAE	0.1	-	-	0.99	137.20	3.90
β -VAE	0.2	-	-	0.99	85.46	3.92
LIDVAE	1.0	0	-	1.00	307.72	3.99
IL-LIDVAE	1.0	0.2	-	1.00	336.86	3.88
IL-LIDVAE	1.0	1.0	-	0.97	458.54	3.84
LRVAE(ours)	1.0	-	0.8	1.00	63.89	3.92

Table 4: Quantitative evaluation on CelebA dataset

wise KL divergence ($KL = D_{KL}(q_\phi(z|x_i)||p(z))$). This KL value indicates average of how far away each latent distribution of sample point is from prior. Too small value means that latent variable is not identifiable with prior. On the other hand, too big value means poor regularization. As we claim, the ideal case is the posterior converges to prior but each latent distribution has moderate KL values. MI denotes mutual information between x_i and z_i . ($MI = I(z, x) = \mathbb{E}_x[\mathbb{E}_{q(z|x)}[q(z|x)]] - \mathbb{E}_x[\mathbb{E}_{q(z|x)}[q(z)]]$). MI indicates correlation between input data and latent variable. These metrics have some limitation to measure every aspect of posterior collapse(especially local posterior collapse), we can see influence in some meaningful aspects from them.

In table 1, we can see evidence that smaller β of β -VAE contributes to reduce posterior collapse on fashionMNIST dataset(Xiao et al., 2017). AU and KL are increased by decreasing β . When the β is 1.0(VAE), AU is 0.13. The AU increases to 0.16, 0.19, and 0.22 when β is decreased to 0.4, 0.2, and 0.1. Thus, reducing β is meaningful influence, but limited. Decreasing β always increases AU. However, be careful that decreasing β also induces poor regularization. LIDVAE and IL-LIDVAE impressively increase AU to 0.42, 0.80, and 0.72 and KL to 25.15, 49.54, 54.58, and 67.35. However these KL values may be too large for regularization. Whereas, our LRVAE also achieves high AU such as 0.95, 0.93, and 0.41 with KL 45.23, 33.36, and 12.41. Although there is no a particular appropriate value, we say that this is an evidence that our method has benefit to avoid posterior collapse with better regularization.

We also evaluate on MNIST(Deng, 2012) as shown in Table 2. Our proposed loss term with a certain importance($\alpha_T = 0.4$) contributes to increase AU from 0.68, 0.38, and 0.16 to 1.00, 0.99, and 0.22 when $\beta = 0.1, 0.2, 1.0$ respectively. We also can see that higher importance($\alpha_T = 1.0$) increases AU again to 0.66 from 0.22.

We can see similar pattern in experiments on Omniglot dataset(Lake et al., 2015) in Table 3. AU of VAE is only 0.06 but this value increases to 0.86 by minimizing latent

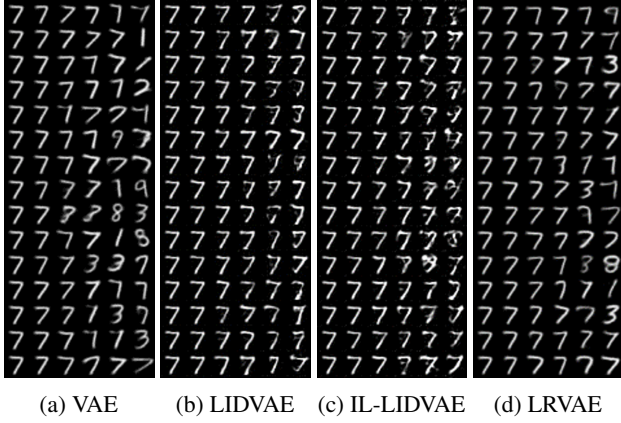


Figure 3: Reconstruction from noised latent vectors results on MNIST dataset: IL-LIDVAE uses $L = 0.2$ and LRVAE uses $\alpha_T = 0.8$.

reconstruction loss($\alpha_T = 1.0$). Reducing importance of regularization loss(β) to 0.1 also achieves similar AU(0.85), but the KL value also increases extremely(2.32 to 30.05). Results of IL-LIDVAE also show huge KL values(109.73, 120.17) while KL of LRVAE is relatively stable(7.84). MI value gradually increases from 2.11 in VAE to 2.76, 3.26, and 3.32 where importance of LR(α_T) increases from 0 to 0.1, 0.4, and 1.0.

Table 4 shows results on CelebA dataset(Liu et al., 2015). Our proposed LR also contribute to increase AU to 1.00 from 0.47 under proper KL value(63.89). On the other hand, LIDVAE and IL-LIDVAE achieve similar AU with KL values which are over 300.

Experiments are conducted to explore the response of decoders to local changes in latent variables as shown in Figure 3. In this figure, MNIST dataset(Deng, 2012) is used. The columns of each sub-figure are the results of decoding the latent vector after adding Gaussian noise with variance of 0.0, 0.2, 0.4, 0.6, 0.8, and 1.0 from the left. That is, the leftmost column of each sub-figure is equal to the pure reconstruction result. In this experiment, all of results in the figure are reconstructed from an exactly same input data point(a handwriting ‘7’). In this experiment, we use shallow structure of only 1,168,641 parameters for VAE and LRVAE, while LIDVAE and IL-LIDVAE have 3,776,658 parameters. Models are trained 100 epochs equally. VAE(3a) generates out of class(1, 3, 8, or, 9) results compared other models. LIDVAE(3b) and IL-LIDVAE(3c) show tendency to produce images with added artifacts rather than normally diverse results. These artifacts are due to the side effect of the network restoration. Whereas, our LRVAE shows better results as shown in Figure 3d.

We provide generation results from randomly sampled latent vectors($z \sim N(0, I)$) in Figure 4. In this experiment,

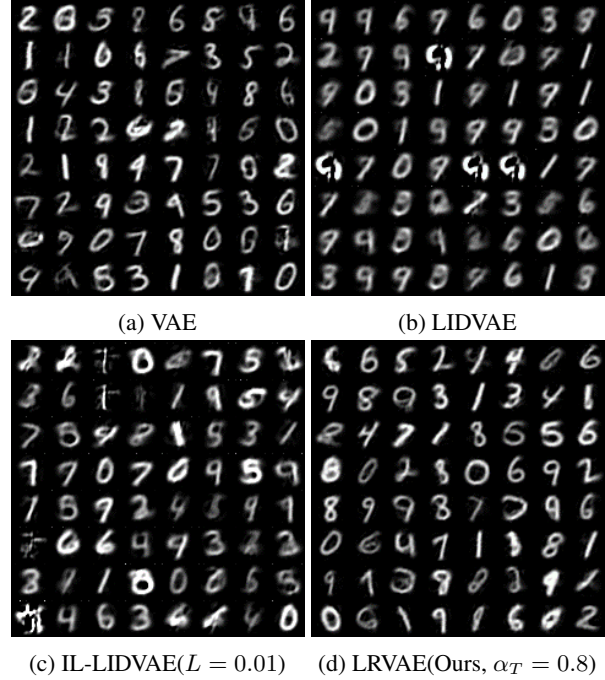


Figure 4: Sampling(Generation) results on MNIST dataset

LIDVAE and IL-LIDVAE have 3,776,658 parameters while β -VAE and LRVAE(ours) have 1,915,792 parameters. In our implementation, LIDVAE and IL-LIDVAE use single Gaussian prior for equal comparison with β -VAE and LRVAE, unlike original implementation(Wang et al., 2021)(Kinoshita et al., 2023) that uses GMVAE(Dilokthanakul et al., 2016). We can see some collapsed outputs and less diversity in LIDVAE(Figure 4b). Diversity can be improved by controlling inverse Lipschitz value L (Figure 4c). However, collapsed outputs are still observed. Strictly restricted network structure has limitation to optimize mapping between complex data distribution and simple prior distribution.

We also have reconstruction experiments with added tiny Gaussian noises on fashionMNIST(Xiao et al., 2017) as shown in Figure 5. VAE and LRVAE share the same network structure and parameters (1,168,641), while LIDVAE and IL-LIDVAE have identical network structures and parameters (3,776,658). Models are trained 100 epochs equally. VAE fails to reconstruct the pants images as shown in (b). The variance of Gaussian noise added increases by 0.5 from the left column to the right column. e.g., noises sampled from $N(0, 3.0I)$ are added to the latent vector for last images. LIDVAE(c) and IL-LIDVAE(d) reconstruct pants, but their outputs are blurry and lack in diversity. Our LRVAE(e) successfully reconstructs the object of the input relatively clearly and showing diversity proportional to magnitude of noise. We test on FFHQ-256(Karras et al., 2019) dataset through VDVAE(Child, 2020) for qualitative evaluation of our proposed approach on large scale and deeper model. We

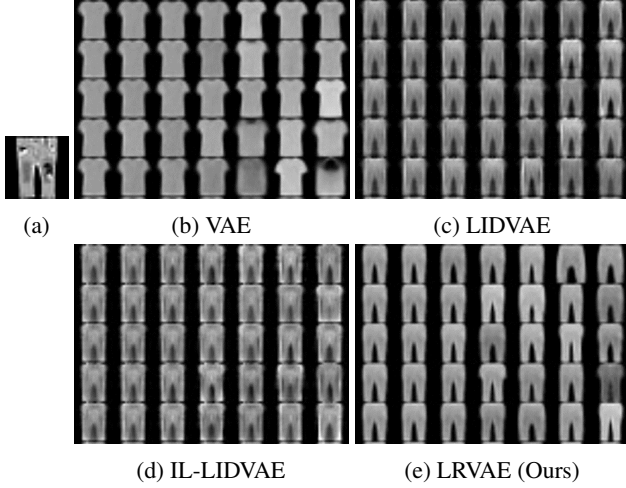


Figure 5: Reconstruction from noised latent vectors on fashionMNIST dataset: (a) is the input image. IL-LIDVAE uses $L = 0.2$ and LRVAE uses $\alpha_T = 1.0$.

fine-tune the VDVAE from pre-trained parameters through additional 50,000 iteration with each different ELBO objectives. In Figure 6, LRVDVAE is trained using proposed ELBO objectives with $\alpha_T = 1.0$, while VDVAE is trained using classical ELBO objectives. Each row shows images which are generated from latent vectors with the addition of four randomly sampled noise vectors from $N(0, 0.0I)$, $N(0, 0.3I)$, and $N(0, 0.4I)$. i.e., the images at first row are equal to the pure reconstruction result.

VDVAE(a) shows little difference among output images despite of added noise. On the other hand, LRVDVAE(b) shows larger variation among output images compared to VDVAE when the noise is sampled from $N(0, 0.3I)$ and $N(0, 0.4I)$. Classical ELBO doesn't enforce the model to identify latent vectors which sampled from same input data. While, proposed ELBO enforces the model to response to small amount change of latent variable revealing improved local identifiability.

5. Conclusion

In this work, we introduce the concept of $\epsilon(x)$ -posterior collapse, a more general and relaxed notion that permits thresholds which vary locally across the data manifold. We further define $L(z)$ -bi-Lipschitz continuity to express a locally elastic constraint on the decoder. We theoretically and empirically demonstrate that enforcing $L(z)$ -bi-Lipschitz continuity helps mitigate $\epsilon(x)$ -posterior collapse. We believe this insight will broaden the practical utility of VAEs by removing unnecessary restrictions. Moreover, we propose Latent Reconstruction(LR) loss as an additional loss to the conventional data reconstruction loss aimed at control posterior collapse by hyper-parameter α_T . Minimizing LR

loss achieves latent identifiability by leading the decoder and encoder to satisfy $L(z)$ -bi-Lipschitz continuity. As a result, the LR loss enables controlling posterior collapse across most VAE architectures. In practice, our method enhances the diversity of the output in local regions while using fewer parameters. In conclusion, our work contributes to a better understanding of posterior collapse and provides a pathway to address it under more practical settings for VAEs.

Despite these advancements, it's important to acknowledge certain limitations of this work. Our analysis indicates that the α value and the local bi-Lipschitz constant $L(z)$ would not be directly proportional. Consequently, for certain datasets and network architectures, a high α might still result in a weakly enforced constraint. While this relaxation is an intended design choice to mitigate side effects from network constraints, it could potentially diminish the effectiveness of preventing posterior collapse in some sce-



(a) VDVAE



(b) LRVDVAE (Ours)

Figure 6: Reconstruction results from noised latent vectors on FFHQ-256 dataset

narios. Furthermore, our theoretical framework assumes that both the DR loss and LR loss can be sufficiently minimized. However, achieving sufficiently low values for both losses simultaneously can be challenging in practice. We hypothesize that a certain degree of invertibility, though not necessarily full invertibility, might be required for both the encoder and decoder to adequately minimize these losses. This aspect was not explored in the current study.

References

- Amos, B., Xu, L., and Kolter, J. Z. Input convex neural networks. In *International conference on machine learning*, pp. 146–155. PMLR, 2017.
- Child, R. Very deep vaes generalize autoregressive models and can outperform them on images. *arXiv preprint arXiv:2011.10650*, 2020.
- Clapham, P. and Grzes, M. Posterior collapse in variational gradient origin networks. In *2023 International Conference on Machine Learning and Applications (ICMLA)*, pp. 980–987. IEEE, 2023.
- Dai, B., Wang, Z., and Wipf, D. The usual suspects? reassessing blame for vae posterior collapse. In *International conference on machine learning*, pp. 2313–2322. PMLR, 2020.
- Dai, B., Wenliang, L., and Wipf, D. On the value of infinite gradients in variational autoencoder models. *Advances in Neural Information Processing Systems*, 34:7180–7192, 2021.
- Deng, L. The mnist database of handwritten digit images for machine learning research [best of the web]. *IEEE signal processing magazine*, 29(6):141–142, 2012.
- Dilokthanakul, N., Mediano, P. A., Garnelo, M., Lee, M. C., Salimbeni, H., Arulkumaran, K., and Shanahan, M. Deep unsupervised clustering with gaussian mixture variational autoencoders. *arXiv preprint arXiv:1611.02648*, 2016.
- He, J., Spokoyny, D., Neubig, G., and Berg-Kirkpatrick, T. Lagging inference networks and posterior collapse in variational autoencoders. *arXiv preprint arXiv:1901.05534*, 2019.
- Higgins, I., Matthey, L., Pal, A., Burgess, C., Glorot, X., Botvinick, M., Mohamed, S., and Lerchner, A. beta-vae: Learning basic visual concepts with a constrained variational framework. In *International conference on learning representations*, 2017.
- Ichikawa, T. and Hukushima, K. Learning dynamics in linear variational autoencoder: Posterior collapse threshold and kl annealing. In *Proceedings of the 27th International Conference on Artificial Intelligence and Statistics (AISTATS)*, 2024. URL <https://proceedings.mlr.press/v238/ichikawa24a.html>.
- Karras, T., Laine, S., and Aila, T. A style-based generator architecture for generative adversarial networks. In *Proceedings of the IEEE/CVF conference on computer vision and pattern recognition*, pp. 4401–4410, 2019.
- Kim, Y., Wiseman, S., Miller, A., Sontag, D., and Rush, A. Semi-amortized variational autoencoders. In *International Conference on Machine Learning*, pp. 2678–2687. PMLR, 2018.
- Kingma, D. P. and Welling, M. Auto-encoding variational bayes. *arXiv preprint arXiv:1312.6114*, 2013.
- Kinoshita, Y. and Toyoizumi, T. A provable control of sensitivity of neural networks through a direct parameterization of the overall bi-lipschitzness. *Advances in Neural Information Processing Systems*, 37:85241–85309, 2024.
- Kinoshita, Y., Oono, K., Fukumizu, K., Yoshida, Y., and Maeda, S.-i. Controlling posterior collapse by an inverse lipschitz constraint on the decoder network. In *International Conference on Machine Learning*, pp. 17041–17060. PMLR, 2023.
- Lake, B. M., Salakhutdinov, R., and Tenenbaum, J. B. Human-level concept learning through probabilistic program induction. *Science*, 350(6266):1332–1338, 2015.
- Liu, Z., Luo, P., Wang, X., and Tang, X. Deep learning face attributes in the wild. In *Proceedings of the IEEE international conference on computer vision*, pp. 3730–3738, 2015.
- Lucas, J., Tucker, G., Grosse, R., and Norouzi, M. Understanding posterior collapse in generative latent variable models. *International Conference on Learning Representations*, 2019a.
- Lucas, J., Tucker, G., Grosse, R. B., and Norouzi, M. Don’t blame the elbo! a linear vae perspective on posterior collapse. *Advances in Neural Information Processing Systems*, 32, 2019b.
- Razavi, A., Oord, A. v. d., Poole, B., and Vinyals, O. Preventing posterior collapse with delta-vaes. *arXiv preprint arXiv:1901.03416*, 2019.
- Rueckert, F. L. et al. Cr-vae: Contrastive regularization on variational autoencoders for preventing posterior collapse. *arXiv preprint arXiv:2309.02968*, 2023.
- Song, Y., Sun, L., and Liu, P. Scale-VAE: Preventing posterior collapse in variational autoencoder. In *Proceedings of the 2024 Joint International Conference on Computational Linguistics (LREC-COLING)*, 2024. URL <https://aclanthology.org/2024.lrec-main.383>.

- Wang, Y., Blei, D., and Cunningham, J. P. Posterior collapse and latent variable non-identifiability. *Advances in Neural Information Processing Systems*, 34:5443–5455, 2021.
- Xiao, H., Rasul, K., and Vollgraf, R. Fashion-mnist: a novel image dataset for benchmarking machine learning algorithms. *arXiv preprint arXiv:1708.07747*, 2017.
- Zhao, S., Song, J., and Ermon, S. Infovae: Balancing learning and inference in variational autoencoders. In *Proceedings of the aaai conference on artificial intelligence*, volume 33, pp. 5885–5892, 2019.

A. Proofs of Main Theorems

A.1. Proof of Theorem 2.3

Theorem A.1 (Gaussian VAE: $L(z)$ -bi-Lipschitz avoids $\epsilon(x)$ -posterior collapse with probability $1 - \zeta$). *Fix a confidence level $\zeta \in (0, 1)$ and let radius R_ζ be defined as in Definition 2.2. Let the prior be $p(z) = \mathcal{N}(0, I)$ and the likelihood*

$$p(x | z) = \mathcal{N}(D_{\hat{\theta}}(z), \sigma^2 I).$$

Assume the decoder $D_{\hat{\theta}}$ is C^2 and $L(z)$ -bi-Lipschitz with probability $1 - \zeta$. Consider any $x \in \mathcal{X}$ for which there exists z_0 satisfying

$$\|z_0\| \leq R_\zeta, \quad D_{\hat{\theta}}(z_0) = x.$$

Define

$$\begin{aligned} \Sigma &= \left(I + \frac{1}{\sigma^2} J_D(z_0)^\top J_D(z_0) \right)^{-1}, \\ \kappa_{\min} &= \sigma_{\min}(J_D(z_0)) \geq \frac{1}{L(z_0)} > 0. \end{aligned}$$

Then, under the Laplace approximation,

$$\begin{aligned} p(z | x) &\approx \mathcal{N}(z_0, \Sigma) \\ \Rightarrow D_{\text{KL}}(p(z | x) \| p(z)) &\geq \frac{C}{2} \log\left(1 + \frac{\kappa_{\min}^2}{\sigma^2}\right) > 0. \end{aligned}$$

Consequently, with probability at least $1 - \zeta$ over $x \sim p_{\text{data}}$, no $\epsilon(x) < \frac{C}{2} \log(1 + \kappa_{\min}^2/\sigma^2)$ can satisfy Definition 2.1.

Proof. We restate the calculation while explicitly conditioning on the high-probability event that defines the *effective support*.

0. Conditioning on the effective support. Let $\mathcal{E}_\zeta := \{\|Z\| \leq R_\zeta\}$ so that $\Pr_{Z \sim p}(\mathcal{E}_\zeta) \geq 1 - \zeta$ by Definition 2.2. Fix any $x \in \mathcal{X}$ for which there exists $z_0 \in \mathcal{E}_\zeta$ satisfying $D_{\hat{\theta}}(z_0) = x$. Because z_0 lies in \mathcal{E}_ζ , the local $L(z)$ -bi-Lipschitz bound $\sigma_{\min}(J_D(z_0)) \geq 1/L(z_0) > 0$ is guaranteed.

1. Laplace approximation of the posterior. Define $\ell(z) = \log p(x, z) = \log p(x | z) + \log p(z)$. A second-order Taylor expansion of $-\ell(z)$ around its mode z_0 gives

$$-\ell(z) \approx \frac{1}{2} (z - z_0)^\top \left(I + \frac{1}{\sigma^2} J_D(z_0)^\top J_D(z_0) \right) (z - z_0) + \text{const},$$

whence $p(z | x) \approx \mathcal{N}(z_0, \Sigma)$ with $\Sigma^{-1} = I + \sigma^{-2} J_D(z_0)^\top J_D(z_0)$.

2. Exact KL divergence between two Gaussians. For any mean-covariance pair (m, Σ) ,

$$D_{\text{KL}}(\mathcal{N}(m, \Sigma) \| \mathcal{N}(0, I)) = \frac{1}{2} (\text{tr}(\Sigma) + m^\top m - \log \det \Sigma - C).$$

Substituting $m = z_0$ and the above Σ yields

$$D_{\text{KL}}(p(z | x) \| p(z)) \approx \frac{1}{2} (\text{tr}(\Sigma) + z_0^\top z_0 - \log \det \Sigma - C).$$

3. Lower bound via the smallest singular value. Because every eigenvalue of Σ^{-1} is at least 1, each eigenvalue of Σ is at most 1, so $\text{tr}(\Sigma) \leq C$. Dropping the non-negative term $z_0^\top z_0$ gives

$$D_{\text{KL}}(p(z | x) \| p(z)) \geq -\frac{1}{2} \log \det \Sigma = \frac{1}{2} \log \det \Sigma^{-1}.$$

Let ς_i be the singular values of $J_D(z_0)$; then the eigenvalues of Σ^{-1} are $\lambda_i = 1 + \varsigma_i^2/\sigma^2$, so, with $\kappa_{\min} := \min_i \varsigma_i \geq 1/L(z_0) > 0$,

$$\begin{aligned} \det(\Sigma^{-1}) &= \prod_{i=1}^C (1 + \varsigma_i^2/\sigma^2) \geq (1 + \kappa_{\min}^2/\sigma^2)^C, \\ D_{\text{KL}}(p(z | x) \| p(z)) &\geq \frac{C}{2} \log(1 + \kappa_{\min}^2/\sigma^2) > 0. \end{aligned}$$

4. Translating the bound to a probabilistic statement. Steps 0–3 hold for every $z_0 \in \mathcal{E}_\zeta$; hence

$$\Pr_{Z \sim p} \left(D_{\text{KL}}(p(z | x) \| p(z)) > 0 \right) \geq 1 - \zeta.$$

Consequently, with the same probability over x induced by the generative process, no $\epsilon(x) < \frac{C}{2} \log(1 + \kappa_{\min}^2 / \sigma^2)$ can satisfy Definition 2.1. This completes the proof. \square

A.2. Proof of Theorem 3.1

Theorem A.2 (High-Probability Locally Bi-Lipschitz under Piecewise-Linear Networks). *Fix confidence levels $\zeta, \varrho \in (0, 1)$ and let radius R_ζ be defined as in Definition 2.2. Let $D_\theta : \mathbb{R}^C \rightarrow \mathbb{R}^D$ and $E_\varphi : \mathbb{R}^D \rightarrow \mathbb{R}^C$ be feed-forward networks built from affine layers and piecewise-linear activations (e.g. ReLU, LeakyReLU).*

Draw $Z \sim p(z)$ and denote the effective-support event $\mathcal{E}_\zeta := \{\|Z\| \leq R_\zeta\}$, which satisfies $\Pr(\mathcal{E}_\zeta) \geq 1 - \zeta$. On \mathcal{E}_ζ there exists a radius $r > 0$ such that the activation pattern of every piecewise-linear unit is fixed on $B(Z, r)$. Hence D_θ and $E_\varphi \circ D_\theta$ restrict to affine maps on $B(Z, r)$ and are therefore \mathcal{C}^1 there.

Define the random variables

$$A := \|J_D(Z)\|_\sigma, \quad B := \|J_{E \circ D}(Z) - I\|_\sigma,$$

and assume $\mathbb{E}[A^2] < \infty$ and $\mathbb{E}[B^2] < \infty$.

Then for any $\varepsilon \in (0, 1)$ there exist thresholds $\tau_r, \tau_l > 0$ (depending on ε, ϱ) such that, if

$$\mathcal{L}_{\text{DR}}(\theta, \varphi) \leq \tau_r, \quad \mathcal{L}_{\text{LR}}(\theta, \varphi) \leq \tau_l,$$

the following holds with probability at least $1 - \zeta - \varrho$ over $Z \sim p$:

There exist constants $L_f < \infty$ and $\eta < 1$ such that

$$A \leq L_f, \quad B \leq \eta,$$

and consequently D_θ is bi-Lipschitz on the ball $B(Z, r)$ with constant

$$L = \max\left(L_f, \frac{1}{1-\eta}\right),$$

i.e. for all $z_1, z_2 \in B(Z, r)$,

$$(1 - \varepsilon) \|z_1 - z_2\| \leq \|D_\theta(z_1) - D_\theta(z_2)\| \leq (1 + \varepsilon) \|z_1 - z_2\|.$$

Proof. **0. Conditioning on the effective support.** Work on the event \mathcal{E}_ζ ; this costs probability at most ζ .

1. Probabilistic bounds on A, B . Since $\mathbb{E}[A^2]$ and $\mathbb{E}[B^2]$ are finite, Markov’s inequality yields constants $L_f < \infty$ and $\eta < 1$ such that

$$\Pr(A > L_f) \leq \frac{\varrho}{2}, \quad \Pr(B > \eta) \leq \frac{\varrho}{2}.$$

By a union bound, with probability at least $1 - \varrho$ (unconditionally) we have $A \leq L_f$ and $B \leq \eta$.

2. Local affine region. For any Z (in fact for all but a measure-zero set) there exists $r > 0$ such that the activation pattern of every piecewise-linear unit is constant on $B(Z, r)$. Consequently,

$$J_D(z) = J_D(Z), \quad J_{E \circ D}(z) = J_{E \circ D}(Z), \quad \forall z \in B(Z, r).$$

3. Lipschitz upper bound. Because D_θ is affine on $B(Z, r)$,

$$\|D_\theta(z_1) - D_\theta(z_2)\| = \|J_D(Z)(z_1 - z_2)\| \leq A \|z_1 - z_2\| \leq (L_f + \varepsilon) \|z_1 - z_2\|.$$

4. Lipschitz lower bound. On the same ball, $\|J_{E \circ D}(Z) - I\|_\sigma = B \leq \eta < 1$, so by the inverse-function theorem for affine maps,

$$\|D_\theta(z_1) - D_\theta(z_2)\| \geq (1 - \eta) \|z_1 - z_2\|.$$

5. Collecting probabilities. Steps 1–4 hold whenever (i) \mathcal{E}_ζ occurs and (ii) the event $\{A \leq L_f, B \leq \eta\}$ occurs. By the union bound the joint probability is at least $1 - \zeta - \varrho$, yielding the desired two-sided inequality with $L = \max(L_f, 1/(1 - \eta))$ and completing the proof. \square

B. Definition List of Posterior Collapse

Table 5: Comparison of posterior collapse definitions across different works.

Work	Definition	Condition	Metric	Locality	Target
(Wang et al., 2021)	$p_{\hat{\theta}}(z x) = p(z)$	Equality	Exact match	Global	$p_{\hat{\theta}}$
(Razavi et al., 2019)	$D_{\text{KL}}(q(z x) \ p(z)) \rightarrow 0$	Vanishing KL	KL divergence	Global	q_φ
(Lucas et al., 2019b)	$\mathbb{P}_{x \sim p(x)}[D_{\text{KL}} < \epsilon] \geq 1 - \Delta$	Probabilistic	KL divergence	Global	q_φ
(Kinoshita et al., 2023)	$d(q_{\hat{\phi}}(z x), p(z)) \leq \epsilon$	Threshold	General divergence	Global	q_φ
Ours	$d(\rho(z x), p(z)) \leq \epsilon(x)$	Functional bound	General divergence	Local	$p_{\hat{\theta}}, q_{\hat{\varphi}}$

Table 5 summarizes several existing definitions of posterior collapse and compares them with our proposed $\epsilon(x)$ -posterior collapse. The earliest work by (Wang et al., 2021) adopts the strongest criterion, defining collapse as exact equality between the true posterior and prior, which excludes even small meaningful variations. Later works (Razavi et al., 2019; Kinoshita et al., 2023) propose divergence-based criteria such as a vanishing KL divergence or a constant threshold ϵ , but still apply the condition uniformly over the input space.

(Lucas et al., 2019b) proposes a probabilistic relaxation, introducing (ϵ, Δ) -posterior collapse, which tolerates deviations on a small subset of the data distribution. However, all of these approaches remain global in their treatment of input samples.

In contrast, our formulation introduces a data-dependent threshold function $\epsilon(x)$ that varies across the domain \mathcal{X} . This allows a flexible treatment of regions with low informativeness (e.g., noise), while maintaining strict identifiability around data points. Additionally, by adopting the true posterior $p(z|x)$ as the target rather than the approximate posterior, our definition enables clearer theoretical analysis and model evaluation. The locality and adaptiveness of our formulation make it both a generalization and refinement of previous definitions.

C. Symmetric loss and mutual information

Theorem C.1 (Latent Reconstruction Loss Tightens a Mutual–Information Lower Bound). *Let the generative joint be $p(z, x) = p(z) p_\theta(x | z)$ with latent prior $p(z)$. For any variational family $q_\varphi(z | x)$ define the latent–reconstruction loss*

$$\mathcal{L}_{\text{LR}}(\theta, \varphi) := \mathbb{E}_{p(z, x)}[-\log q_\varphi(z | x)].$$

Then the following decomposition holds:

$$\boxed{\mathcal{L}_{\text{LR}}(\theta, \varphi) = H(Z | X) + \mathbb{E}_{p(x)}[D_{\text{KL}}(p(z | x) \| q_\varphi(z | x))]} \quad (3)$$

Consequently,

$$\mathcal{L}_{\text{LR}}(\theta, \varphi) \geq H(Z | X) = H(Z) - I(Z; X), \quad (4)$$

with equality iff $q_\varphi(z | x) = p(z | x)$ almost surely. Hence minimizing \mathcal{L}_{LR} (i) tightens the variational posterior toward the true one and (ii) maximizes a lower bound on the mutual information:

$$I(Z; X) \geq H(Z) - \mathcal{L}_{\text{LR}}(\theta, \varphi). \quad (5)$$

Proof. Let $p(z, x) = p(z)p_\theta(x | z)$ and abbreviate $q(z | x) := q_\varphi(z | x)$.

$$\begin{aligned}\mathcal{L}_{\text{LR}} &= \mathbb{E}_{p(z, x)}[-\log q(z | x)] = \mathbb{E}_{p(x)}\mathbb{E}_{p(z|x)}[-\log q(z | x)] \\ &= \mathbb{E}_{p(x)}[H_{p, q}(Z | X=x)] \quad (\text{cross entropy}) \\ &= \mathbb{E}_{p(x)}[H(Z | X=x) + D_{\text{KL}}(p(z | x) \| q(z | x))] \\ &= H(Z | X) + \mathbb{E}_{p(x)}[D_{\text{KL}}(p(z | x) \| q(z | x))],\end{aligned}$$

which is identity (1). The KL term is non-negative, giving the inequality (2). Since $H(Z | X) = H(Z) - I(Z; X)$, rearranging yields the lower bound (3). The KL term vanishes exactly when $q(z | x) = p(z | x)$ a.s., proving tightness. \square

Equation (3) shows that the latent-reconstruction loss naturally decomposes into two terms: (i) the *intrinsic* uncertainty $H(Z | X)$ imposed by the generative model and (ii) an *encoder-mismatch penalty* $\mathbb{E}_{p(x)}[D_{\text{KL}}(p(z | x) \| q_\varphi(z | x))]$. Minimizing \mathcal{L}_{LR} therefore tightens $q_\varphi(z | x)$ toward the true posterior while driving up the lower bound $H(Z) - \mathcal{L}_{\text{LR}}$ on the mutual information $I(Z; X)$. In practical terms, LR loss promotes *information-rich latents* without requiring explicit mutual-information estimators such as MINE. When combined with the ELBO (or DR loss), LR acts as a principled counterpart to the KL term: it reduces posterior collapse by explicitly rewarding cycle consistency $z \rightarrow x \rightarrow \hat{z}$ in latent space, which the standard ELBO is blind to. Empirically (Section 4, Fig. 5), increasing the LR coefficient raises measured $I(Z; X)$ and narrows the gap to the theoretical bound, demonstrating that the inequality in (3) is not only tight in theory (equality when $q_\varphi = p$) but also *practically tight* for well-trained models. This connection provides a clear design principle:

$$\text{Lower } \mathcal{L}_{\text{LR}} \implies \text{Higher } I(Z; X),$$

making LR loss a simple yet powerful lever for controlling the information capacity of VAEs.

D. Symmetric loss and invertibility

Theorem D.1. Let $p_\theta(x|z)$ be a likelihood model and $q_\varphi(z|x)$ an approximate posterior (encoder), with latent prior $p(z)$. Assume that the following losses are minimized for all $x \in \mathcal{X}$:

$$\begin{aligned}\mathcal{L}_{\text{DR}}(x) &:= \mathbb{E}_{q_\varphi(z|x)}[-\log p_\theta(x|z)], \\ \mathcal{L}_{\text{LR}}(x) &:= \mathbb{E}_{p_\theta(x|z)}[-\log q_\varphi(z|x)].\end{aligned}$$

Then, under regularity conditions (smoothness, boundedness, and support alignment), the divergence between the approximate posterior and the true posterior vanishes:

$$d(q_\varphi(z|x), p_\theta(z|x)) \rightarrow 0,$$

for suitable divergences $d(\cdot, \cdot)$, such as the KL divergence or Wasserstein distance.

Proof. From Bayes' rule, we write:

$$p_\theta(z|x) = \frac{p_\theta(x|z)p(z)}{p_\theta(x)}.$$

Assume $p(z)$ and $p_\theta(x|z)$ are smooth and strictly positive, and that $q_\varphi(z|x)$ has support overlapping with $p_\theta(z|x)$.

Step 1 (DR loss): Minimizing

$$\mathcal{L}_{\text{DR}}(x) = \mathbb{E}_{q_\varphi(z|x)}[-\log p_\theta(x|z)]$$

encourages $q_\varphi(z|x)$ to assign high mass where $p_\theta(x|z)$ is large, thus concentrating near modes of $p_\theta(x|z)$.

Step 2 (LR loss): Minimizing

$$\mathcal{L}_{\text{LR}}(x) = \mathbb{E}_{p_\theta(x|z)}[-\log q_\varphi(z|x)]$$

encourages $q_\varphi(z|x)$ to be large in regions where $p_\theta(x|z)$ is large, thus promoting matching with $p_\theta(z|x)$.

Step 3 (Combined loss): The symmetric loss is

$$\mathcal{L}_{\text{Sym}}(x) := \mathcal{L}_{\text{DR}}(x) + \mathcal{L}_{\text{LR}}(x),$$

which satisfies:

$$\mathcal{L}_{\text{Sym}}(x) = \mathbb{E}_{q_\varphi(z|x)}[-\log p_\theta(x|z)] + \mathbb{E}_{p_\theta(x|z)}[-\log q_\varphi(z|x)].$$

If this is minimized, and both expectations are finite, then the overlap between $q_\varphi(z|x)$ and $p_\theta(z|x)$ must be strong.

Step 4 (Divergence bound): For instance, the KL divergence can be bounded:

$$D_{\text{KL}}(q_\varphi(z|x)||p_\theta(z|x)) \leq \mathcal{L}_{\text{Sym}}(x) - H(p_\theta(z|x)),$$

where $H(p_\theta(z|x))$ is constant in φ . Hence, minimizing \mathcal{L}_{Sym} leads to small divergence.

Therefore, minimizing both \mathcal{L}_{DR} and \mathcal{L}_{LR} encourages $q_\varphi(z|x) \rightarrow p_\theta(z|x)$, implying the approximation quality improves and posterior collapse is unlikely to occur. \square

An accurate approximation of $q_\varphi(z|x) \rightarrow p_\theta(z|x)$ also encourages invertibility. We also show the invertibility from a function point of view as follows.

Theorem D.2 (Symmetric Reconstruction Loss Promotes Local Invertibility). *Let the encoder $E_\varphi : \mathcal{X} \rightarrow \mathcal{Z}$ and decoder $D_\theta : \mathcal{Z} \rightarrow \mathcal{X}$ define conditional distributions $q_\varphi(z|x)$ and $p_\theta(x|z)$ with Lipschitz-continuous means and uniformly bounded variances. We refer to the combination of data reconstruction loss and latent reconstruction loss as the symmetric reconstruction loss:*

$$\begin{aligned} \mathcal{L}_{\text{Sym}}(x) &:= \mathcal{L}_{\text{DR}}(x) + \mathcal{L}_{\text{LR}}(x) \\ &= \mathbb{E}_{q_\varphi(z|x)}[-\log p_\theta(x|z)] + \mathbb{E}_{p_\theta(x|z)}[-\log q_\varphi(z|x)]. \end{aligned}$$

Then, minimizing $\mathcal{L}_{\text{Sym}}(x)$ encourages the decoder D_θ and encoder E_φ to satisfy locally inverse Lipschitz continuity:

$$\begin{aligned} \|z_i - z_j\| &\leq L(z_i, z_j) \cdot \|D_\theta(z_i) - D_\theta(z_j)\|, \\ \|x_i - x_j\| &\leq L(x_i, x_j) \cdot \|E_\varphi(x_i) - E_\varphi(x_j)\|, \end{aligned}$$

for some functions $L : \mathcal{Z} \times \mathcal{Z} \rightarrow \mathbb{R}_+$ and $L : \mathcal{X} \times \mathcal{X} \rightarrow \mathbb{R}_+$.

Proof. We analyze each component of \mathcal{L}_{Sym} .

(1) Data reconstruction loss $\mathcal{L}_{\text{DR}}(x)$:

$$\mathcal{L}_{\text{DR}}(x) = \mathbb{E}_{q_\varphi(z|x)}[-\log p_\theta(x|z)].$$

This loss is minimized when $x \approx D_\theta(z)$ for $z \sim q_\varphi(z|x)$. Under bounded variance, we approximate $z \approx \mu_\varphi(x)$, so $x \approx D_\theta(\mu_\varphi(x))$.

Take two distinct inputs x_i, x_j , and define $z_i := \mu_\varphi(x_i)$, $z_j := \mu_\varphi(x_j)$. Good reconstruction requires

$$D_\theta(z_i) \approx x_i, \quad D_\theta(z_j) \approx x_j.$$

Thus, if $z_i \neq z_j$ but $D_\theta(z_i) \approx D_\theta(z_j)$, then $x_i \approx x_j$, contradicting the assumption. Therefore, to maintain accurate reconstructions, the decoder must satisfy:

$$\|z_i - z_j\| \leq L(z_i, z_j) \cdot \|D_\theta(z_i) - D_\theta(z_j)\|$$

for some function $L(z_i, z_j) \in \mathbb{R}_+$. That is, D_θ is locally inverse Lipschitz continuous.

(2) Latent reconstruction loss $\mathcal{L}_{\text{LR}}(x)$:

$$\mathcal{L}_{\text{LR}}(x) = \mathbb{E}_{p_\theta(x|z)}[-\log q_\varphi(z|x)].$$

This loss is minimized when $z \approx \mu_\varphi(x)$ for $x \sim p_\theta(x|z)$. Since $x \approx D_\theta(z)$ under bounded variance, define $x_i := D_\theta(z_i)$, $x_j := D_\theta(z_j)$.

To minimize the loss, we must have:

$$E_\varphi(x_i) \approx z_i, \quad E_\varphi(x_j) \approx z_j.$$

Thus, if $\|z_i - z_j\|$ is large but $\|E_\varphi(x_i) - E_\varphi(x_j)\|$ is small, $q_\varphi(z|x)$ becomes ambiguous and the loss increases.

To avoid this, the encoder must satisfy:

$$\|x_i - x_j\| \leq L(x_i, x_j) \cdot \|E_\varphi(x_i) - E_\varphi(x_j)\|$$

for some function $L(x_i, x_j) \in \mathbb{R}_+$. That is, E_φ is locally inverse Lipschitz continuous.

Minimizing \mathcal{L}_{Sym} ensures that both encoder and decoder avoid collapsing distinct inputs to similar outputs. This enforces local inverse Lipschitz continuity in both directions. \square

E. Notation

Table 6 collects the main symbols and conventions used throughout this paper. Unless stated otherwise, uppercase letters denote random variables, lowercase letters denote deterministic quantities, and $\|\cdot\|_\sigma$ designates the matrix spectral norm. All expectations are taken with respect to the indicated distribution.

Table 6: Summary of notation

Symbol	Meaning / role
$x \in \mathcal{X}$	Input sample (data space)
$z \in \mathcal{Z}$	Latent variable
$p(z)$	Prior over z (standard normal)
$q_\phi(z x)$	Encoder / approximate posterior
$D_\theta(z)$	Decoder network
$E_\phi(x)$	Deterministic encoder branch
$J_D(z)$	Jacobian of D_θ at z
$J_{E \circ D}(z)$	Jacobian of $E_\phi \circ D_\theta$ at z
$A = \ J_D(Z)\ _\sigma$	Spectral norm of decoder Jacobian (r.v.)
$B = \ J_{E \circ D}(Z) - I\ _\sigma$	Spectral deviation of composite Jacobian (r.v.)
L_{DR}	Data reconstruction loss
L_{LR}	Latent reconstruction loss
τ_r, τ_ℓ	Loss thresholds s.t. $L_{DR} \leq \tau_r, L_{LR} \leq \tau_\ell$
$\zeta \in (0, 1)$	Confidence level for effective-support event E_ζ
$\varrho \in (0, 1)$	Auxiliary confidence level (Markov bound)
R_ζ	Radius with $\Pr(\ Z\ \leq R_\zeta) \geq 1 - \zeta$
E_ζ	Effective-support event $\{\ Z\ \leq R_\zeta\}$
r	Local radius (fixed activation pattern)
L_f	Upper bound on $\ J_D(Z)\ _\sigma$ in E_ζ
η	Upper bound on $\ J_{E \circ D}(Z) - I\ _\sigma$ in E_ζ
$L(z)$	Point-wise(local) bi-Lipschitz constant of D_θ
$\epsilon(x)$	Threshold in $\epsilon(x)$ -posterior collapse definition